J Mater Sci (2010) 45:2798–2807
DOI 10.1007/s10853-010-4269-y

Deformation behavior of spray-formed hypereutectic Al–Si alloys

C. Cui · A. Schulz · J. Epp · H. W. Zoch

Received: 14 July 2009 / Accepted: 26 January 2010 / Published online: 9 February 2010

Abstract The deformation behavior of spray-formed hypereutectic aluminum–silicon alloys—AlSi*x* ($x = 18$, 25, and 35 wt%)—has been studied by means of compression test at various temperatures and strain rates. The flow stress of the spray-formed Al–Si alloys increases with decreasing compression temperature and increasing strain rate. Higher silicon content in the alloys also leads to higher flow stress during deformation. The flow curves determined from the compression tests exhibit that the deformation of the materials is controlled by two competing mechanisms: strain hardening, and flow softening. Particle damage during the deformation may have an influence on the flow curves of the alloys with large silicon particles. Based on the flow curves obtained from the compression tests and knowledge of aluminum extrusion, the spray-formed hypereutectic Al–Si alloy billets have been hot extruded into wires with a high area reduction ratio around 189. Since primary silicon particles were greatly refined and uniformly distributed in the spray-formed materials, the heavy deformations of the spray-formed Al–Si alloys containing high amount of silicon were successfully performed.

Introduction

Hypereutectic Al–Si alloys are very interesting materials for automotive, electrical, aeronautic, and astronautic applications due to attractive properties such as low density, high stiffness, good wear resistance, and low coefficient of thermal expansion [1]. These properties can be improved by further increasing silicon content of the materials. However, this leads to coarse microstructures, inherent brittleness, and poor workability when conventional methods are applied to produce such alloys [2, 3]. Spray forming is a relatively new approach for the manufacture of advanced materials with enhanced properties and performances [4–7]. Uniform distribution of refined primary silicon particles and modified eutectic phase can be obtained in the spray-formed hypereutectic Al–Si alloys due to copious nucleation in the melt during rapid cooling in flight and on deposition, the deformation and fragmentation experienced by the partially solidified droplets on impact, and remelting of the solid component of the spray in the top surface region of the deposit [8–11]. Epitaxial growth of eutectic silicon on the pre-existing primary silicon may also contribute to the modification of eutectic phase [12, 13]. The fine and homogeneous microstructures of the spray-formed hypereutectic Al–Si alloys are expected to contribute to good deformability of the materials.

Despite many investigations on the processing, microstructures, and mechanical properties of the spray-formed hypereutectic Al–Si alloys, fundamental study of the deformation behavior of the alloys is rarely seen. The aim of this study is to examine the deformability of spray-formed hypereutectic Al–Si alloys by means of compression test. Based on the flow curves obtained from the compression tests and knowledge of aluminum extrusion, heavy deformation of the spray-formed billets has also been carried out using hot extrusion. The correlation between the deformation behavior and the microstructures of the spray-formed Al–Si alloys is discussed.

C. Cui (✉) · A. Schulz · J. Epp · H. W. Zoch
Foundation Institute of Materials Science, Badgasteiner Str. 3, 28359 Bremen, Germany
e-mail: cscui@iwt.uni-bremen.de

Experimental

Spray forming

In this study, three hypereutectic binary Al–Si alloys containing 18, 25, and 35 wt% silicon respectively were selected as the experimental materials. The spray-forming experiments were performed at the spray-forming facility SK2 at the University of Bremen, Germany. Commercially pure aluminum ingots and silicon particulates were melted in an induction furnace with a nitrogen atmosphere. The molten alloys with a temperature of superheat of 75 K were atomized by a scanning free fall atomizer using nitrogen at a pressure of 0.4–0.6 MPa. The diameter of the pouring nozzle for the melts was 4 mm. Cylindrical billets were spray formed on rotating substrates with a tilting angle of 35°. The spray distance from the top surface of a growing billet to the atomizer was kept constant at about 440 mm during spray-forming process by adjusting the withdrawing speed of the substrate in the range of 0.5–1.0 mm/s. The diameter of the spray-formed billets is in the range of 130–160 mm. The height of the billets is in the range of 400–500 mm.

Compression test

The compression test, in which a cylindrical specimen is upset into a flat pancake, is usually considered as a standard bulk workability test. The average stress state during testing is similar to that in many bulk deformation processes such as forging and extrusion. In order to investigate the deformability of the spray-formed hypereutectic Al–Si alloys, compression tests were carried out on cylindrical specimens taken from the interior of the spray-formed billets. The equipment used to conduct these tests was a deformation dilatometer (Type 805d, Bähr Thermoanalyse). A cylindrical specimen with a diameter of 5 mm and a length of 10 mm is positioned inside an inductive coil by two ceramic holders. Between the specimen and the holders, small molybdenum platens are positioned to reduce friction at the specimen–platen interfaces during its deformation to minimize barreling. The temperature of the specimen is measured by a pair of type K thermocouples welded onto its surface.

The deformation test can be conducted at temperatures up to 1500 °C with the used dilatometer. The inductive coil enables heating rate up to 100 K/s for the specimen, while a nitrogen gas injection cooling system can provide cooling rate up to 100 K/s. The deformation dilatometer can be used with a maximal compression force of 25 kN at constant strain rates between 0.01 and 15 s^{-1}. The minimum residual length of the specimen is 3 mm, and the length change can be realized with a precision of 0.05 µm.

In this study, a series of compression tests were conducted over the temperature ranging from 300 to 500 °C. The specimens were heated at a rate of 5 K/s to the temperature of deformation, then held for 3 min prior to deformation. After deformation, the specimens were cooled down to room temperature at a rate of 3 K/s. The strain rate was controlled to be constant in the range, 0.01–7.5 s^{-1} in the compressive test. For all the tests, the deformation was finished at a true strain value of 0.9. The true strain and the strain rate are calculated according to the following formulas [14, 15]:

$$\varepsilon = \ln\left(\frac{l_0}{l}\right) \tag{1}$$

$$\dot{\varepsilon} = \frac{d\varepsilon}{dt} \tag{2}$$

where ε is the true strain, l_0 the initial length of the specimen before compression, l the length of the specimen at any instant during compression, $\dot{\varepsilon}$ is the true strain rate, and t is the time.

True stress σ is given by the load P divided by the instantaneous cross-sectional area A of the specimen:

$$\sigma = \frac{P}{A} = \frac{4P}{\pi D^2} = \frac{4Pl}{\pi D_0^2 l_0} \tag{3}$$

where D is the instantaneous diameter of the specimen, and D_0 is the initial diameter.

Hot extrusion

In order to eliminate porosity and prepare semi-finished materials for subsequent application, the spray-formed Al–Si alloy billets usually need to be hot worked. Extrusion is one of the common methods for the hot working of aluminum alloys. Indirect hot extrusion was carried out in an experimental 8 MN press at the Extrusion Research and Development Center of the Technical University of Berlin (see Fig. 1). Before extrusion, the spray-formed billets were machined into cylinders with a diameter of 107 mm and a maximum length of 345 mm. Based on the flow curves determined from the compression test and knowledge of aluminum extrusion, the hot extrusion procedures were determined as follows: each billet was heated in an induction furnace to a temperature of 460–470 °C and indirectly extruded to wires of a diameter of 8 mm. Thus, the total area reduction ratio (extrusion ratio) was about 189. The main process parameters of the representative extrusions are listed in Table 1. The extrusion forces for the three different Al–Si alloys were far below the capacity of the press.

Material analysis

Optical microscopy (Axiophot, ZEISS) was conducted on the as-deposited samples (taken from the interior of the

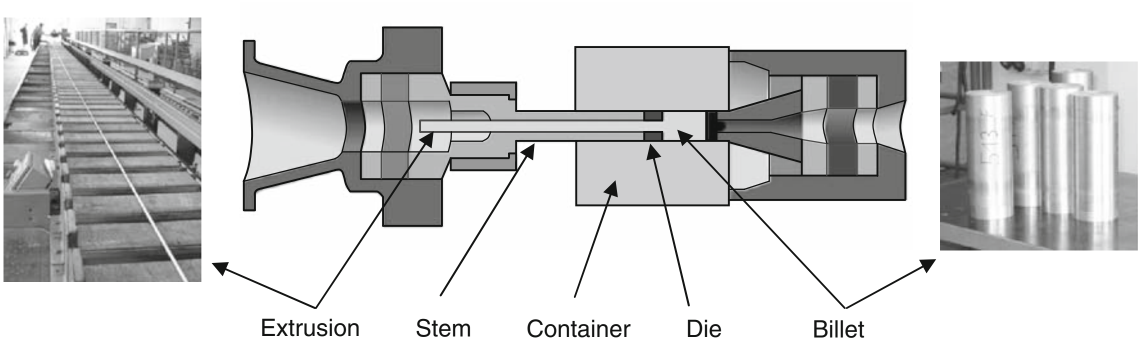

Fig. 1 Indirect extrusion of spray-formed hypereutectic Al–Si alloy billets at the Research Center of Extrusion at the Technical University of Berlin

Table 1 Main extrusion parameters for representative spray-formed Al–Si alloys

Alloy	Billet diameter (mm)	Extrusion diameter (mm)	Extrusion temperature (°C)	Ram speed (mm/s)	Extrusion ratio	Extrusion force (MN)
AlSi18	107	1 × Ø 8	460	0.4	189	3.7
AlSi25	107	1 × Ø 8	465	0.5	189	4.3
AlSi35	107	1 × Ø 8	470	0.4	189	5.1

spray-formed billets, showing the typical microstructures of the materials) and the as-extruded wires. No etching is required as Si appears gray, while the α-Al appears bright.

Results and discussion

Spray-formed materials

The size, morphology, and distribution of silicon phase in the representative spray-formed Al–Si alloys are shown in Fig. 2. The silicon phase in the spray-formed AlSi18 and AlSi25 alloys is very fine (smaller than 5 μm) and granular, indicating the characteristics of spray-formed materials. The silicon phase in the spray-formed AlSi35 alloy is larger than the formers, approximately 10 μm in size. Compared to the phases in the spray-formed alloys, the silicon phase in materials made by low solidification rate process such as conventional casting are much larger, usually with sizes of the order of dozens or hundreds of microns [16]. These large silicon phases are normally in the shapes of blocks, plates, or needles, which are very detrimental to the properties of the materials. The second feature of the spray-formed hypereutectic Al–Si alloys is the homogeneous distribution of silicon phases. Significant differences in the size, shape, and amount of silicon phases have not been observed in the billets except at the outmost surface area. The third obvious difference between the spray-formed materials and the cast materials is the morphology of eutectic phase. The acicular eutectic structure in conventional cast Al–Si alloys seems to be at variance with short and blunted particle structure in the corresponding spray-formed alloys. The significantly refined and modified silicon phases as well as the uniform distribution of the phases can improve the deformability of the materials.

Flow curves

In the deformation during the compression tests, no visible cracks or other defects were initiated in the spray-formed AlSi18 and AlSi25 specimens. This indicates very good deformability of these two materials. The spray-formed AlSi35 specimens also exhibit good deformability in the compression tests. Cracking happened with the AlSi35 specimens at high strain rate 7.5 s^{-1} only at compression temperatures below 400 °C.

A true stress–strain curve is frequently called a flow curve because it gives the stress required for the material to flow plastically to any given strain. The representative flow curves determined from the compression tests of the spray-formed hypereutectic Al–Si alloys are shown in Fig. 3. In general, the flow stress value first increases to reach a maximum value, and then decreases gradually until a true strain value of 0.85 where a small increase appears. Only at high deformation temperatures and low strain rates, the flow stress increases with the strain continually. Decreasing the compression temperature and increasing the strain rate results in high levels of flow stress.

The flow stress values obtained for a true strain of 0.5 at various temperatures and strain rates are plotted and compared in Fig. 4 to find the influence of compression parameters on the deformation behavior of the spray-

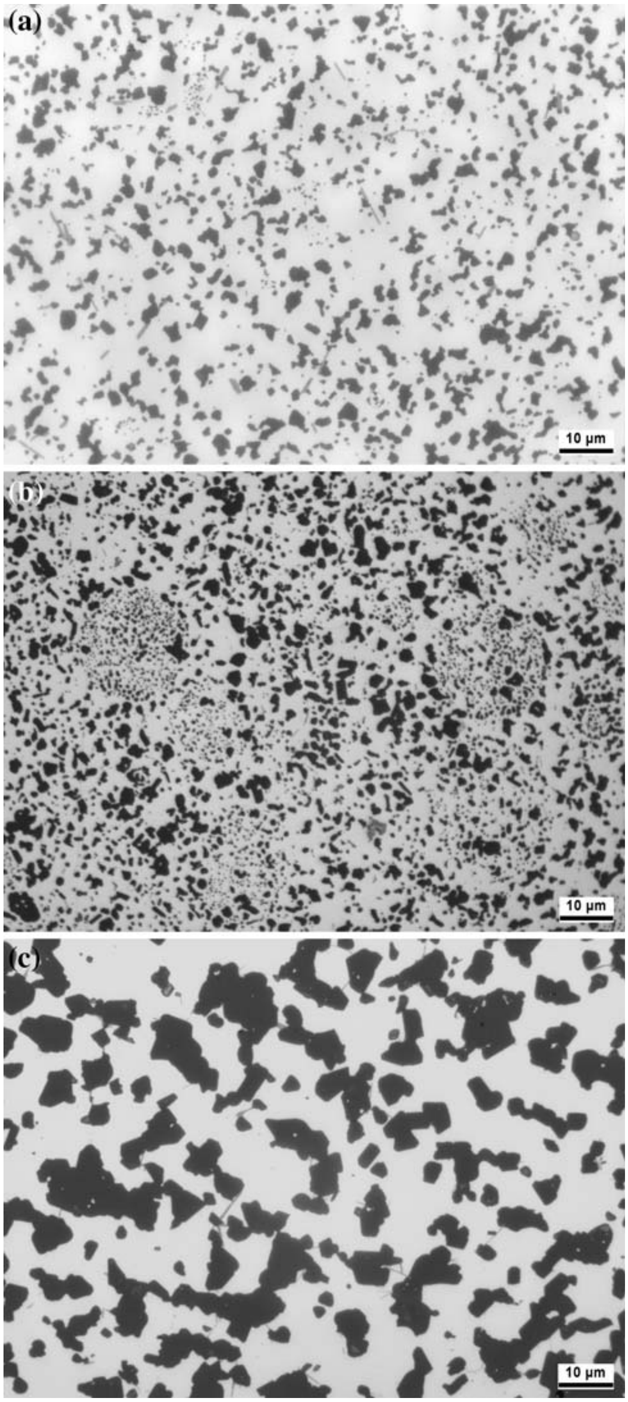

Fig. 2 Microstructures of spray-formed hypereutectic Al–Si alloys: **a** AlSi18; **b** AlSi25; and **c** AlSi35

formed hypereutectic Al–Si alloys. It is shown that at a constant strain rate, increasing compression temperature causes a decrease of the flow stress. On the other hand, increasing strain rate at a constant temperature leads to an increase of the flow stress. The flow stress also increases with increasing silicon content of the materials.

At a constant temperature and strain, a relationship between flow stress and strain rate of a workpiece material undergoing hot deformation can be represented by [14, 15]

$$\sigma = K \times \dot{\varepsilon}^{m} \tag{4}$$

where σ is the flow stress, K a constant, $\dot{\varepsilon}$ the true strain rate, and m the strain rate sensitivity given by

$$m = \partial(\log\sigma)/\partial(\log\dot{\varepsilon}) \tag{5}$$

The calculation of the strain rate sensitivity m allows for finding the effect of the strain rate on the flow stress. The strain rate sensitivity is defined as the slope of the log-stress versus log-strain rate curve for each temperature. For AlSi18, the m value is 0.06 at 300 °C and increases progressively with the temperature up to 0.18 at 500 °C. For AlSi25, the m value falls in the same range and changes in the same way with the temperature. For AlSi35, the m value increases with the temperature, but it is comparatively lower than the other two alloys (as seen in Fig. 5). High m value indicates good deformability of a material.

During plastic deformation there is a generation, movement, and interaction of dislocations. The greater the degree of deformation, the larger the number of dislocations produced. Larger forces are required for further plastic flow due to the interaction and obstruction of the dislocations. This process is generally called work hardening [14, 15].

Another phenomenon flow softening, or work hardening removal, is also frequently observed in deformation. This is mainly caused by thermally activated processes such as dynamic recovery, dynamic recrystallization, and grain growth [14, 15].

Work hardening and flow softening are two competing mechanisms that are concurrent in the compression tests of the spray-formed hypereutectic Al–Si alloys (see Fig. 3). The continuous increase of flow stress with strain at high temperatures and low strain rates indicate that the work hardening rate is slightly higher than the flow softening rate. For the curves that present an almost flat shape, a balance would have been established between the tendency to work harden and the tendency to soften. At high strain rates and low temperatures, the curves present a maximum flow stress peak followed by a reduction. This means that work hardening is the dominant mechanism in the beginning of the deformation, and later flow softening is more active due to possible dynamic recovery, recrystallization, or particle damage.

It is generally recognized that dynamic recrystallization in aluminum alloys does not occur easily during hot deformation in view of their high stacking-fault energy, and dynamic recovery is the predominantly used softening mechanism [15, 17]. However, it is widely confirmed that

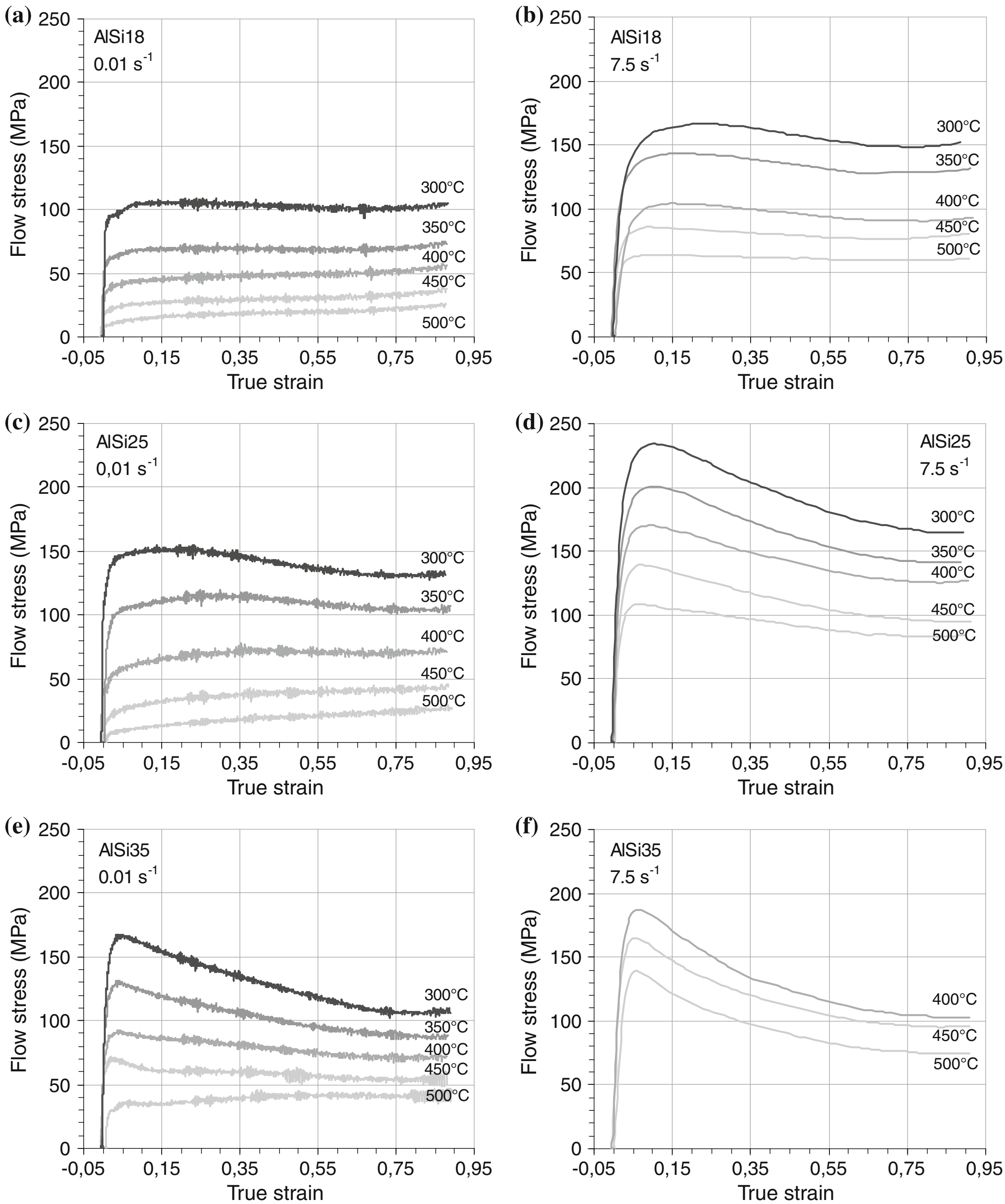

Fig. 3 Flow curves of spray-formed hypereutectic Al–Si alloys determined by compression tests at various temperatures and strain rates: **a** AlSi18, strain rate 0.01 s^{-1}; **b** AlSi18, strain rate 7.5 s^{-1}; **c** AlSi25, strain rate 0.01 s^{-1}; **d** AlSi25, strain rate 7.5 s^{-1}; **e** AlSi35, strain rate 0.01 s^{-1}; and **f** AlSi35, strain rate 7.5 s^{-1}

the addition of ceramic reinforcements to aluminum alloys promote dynamic recrystallization during hot deformation due to very high dislocation density in the vicinity of the hard particles [18–20]. The spray-formed hypereutectic Al–Si alloys can be regarded as composite materials, in which silicon phases act as reinforcement in the α-aluminum matrix. Dynamic recrystallization has also been observed in the hot compressed samples in this study. Figure 6 shows the grain structures of the spray-formed AlSi25 alloy before and after compression test. Significant grain refinement can be seen in the alloy after the hot deformation.

The presence of a high volume fraction of uniformly dispersed hard particles greatly increases the flow stress

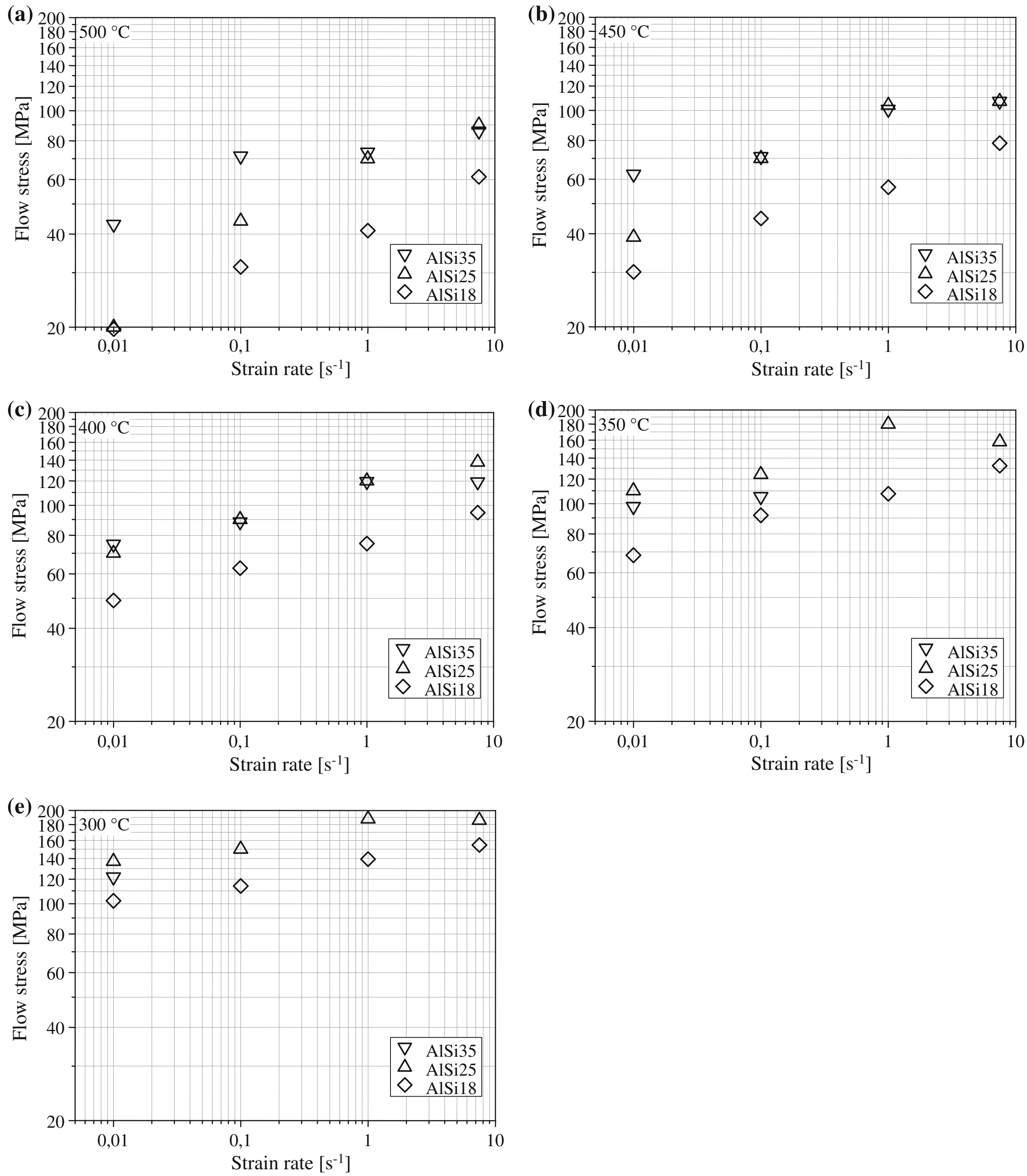

Fig. 4 Flow stress of spray-formed hypereutectic Al–Si alloys as a function of strain rate at various compression temperatures (at the true strain of 0.5): **a** 500 °C; **b** 450 °C; **c** 400 °C; **d** 350 °C; and **e** 300 °C

and makes the deformation difficult. If the second-phase particles are hard and more massive, they will tend to fracture on deformation with the softer matrix extruding into the voids created by this fracturing [15]. Therefore, this type of particle damage also plays a role in the deformation behavior of the materials [21–23]. The microscopic study of the spray-formed Al–Si alloys before and after the compression test showed that only the relatively large silicon particles in the AlSi35 samples suffer obvious fracture. Small silicon particles in the AlSi18 and AlSi25 samples essentially retain their shape and size after the compression. Particle damage during the deformation

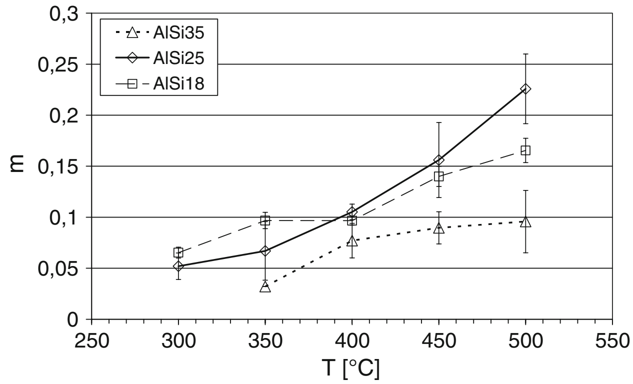

Fig. 5 Variation of strain rate sensitivity m with deformation temperature T at the true strain of 0.5

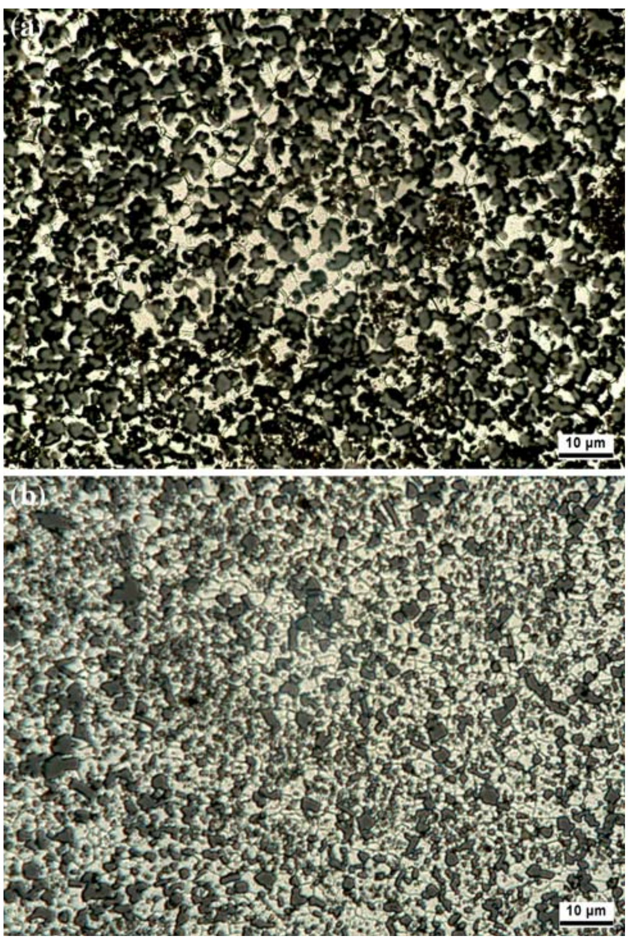

Fig. 6 Grain structures of spray-formed hypereutectic AlSi25 alloy: **a** before compression; and **b** after compression at 500 °C, strain 0.9, and strain rate 0.01 s^{-1}

may have an influence on the flow curves of the alloys with large silicon particles. A dramatic drop in the flow stresses, following the peaks of the curves, can be seen in Fig. 3f.

The decrease of the flow stress with increasing temperature is essentially the consequence of the increase of the diffusion, and, therefore, thermally activated dislocation movement increases. The stress required to deform the material becomes lower.

The strain rate affects the flow stress through the time- and temperature-dependent dynamic recovery and recrystallization. At high strain rates, the time for dynamic recovery and recrystallization may be insufficient. The flow stress increases with the strain rate since work hardening rate becomes more pronounced than flow softening.

The flow stress values of the alloys containing higher levels of silicon are higher because of the presence of larger amount of silicon particles in the aluminum matrix. These reinforcements (silicon particles) would obstruct the movement of dislocations more efficiently and, therefore, it is more difficult for plastic deformation to proceed.

Extrusion

On the basis of flow curve determination, the extrusion force required for the indirect extrusion of the spray-formed hypereutectic Al–Si alloys can be calculated by [24]

$$F = \frac{A_0 \cdot k_f \cdot \varphi_h}{\eta_F} \tag{6}$$

where F is the extrusion force, A_0 is the initial cross-sectional area of the extrusion, k_f is the uniaxial flow stress at the conditions of temperature and strain rate used during extrusion, and φ_h is the total strain defined by

$$\varphi_h = \ln\frac{A_0}{A_f} \tag{7}$$

where A_f is the cross-sectional area after extrusion. η_F is a deformation coefficient accounting for nonhomogeneous deformation of the billet and die friction, frequently in the range of 0.4–0.6.

For indirect extrusion, the strain rate of the extrusion can be approximately calculated according to [24]

$$\dot{\varphi} = \frac{6 \cdot v_{st} \cdot \varphi_h}{D} \tag{8}$$

where v_{st} is the ram speed, and D is the inner diameter of the container.

Under the extrusion conditions in this study, one can calculate that the total strain of the spray-formed hypereutectic Al–Si alloy billets is about 5.24, and the strain rate is in the range of 0.11–0.14. At this strain rate and the extrusion temperature of 460–470 °C, the flow stress values of the three alloys AlSi18, AlSi25, and AlSi35 are found in the range of 45–70 MPa according to their flow curves. If the deformation coefficient η_F is set to 0.6, the extrusion forces are estimated to be in the range of

3.7–5.8 MN. This estimation fits the experimental results quite well (Table 1).

By means of the above described procedure, one can also predict the extrusion force required for the spray-formed Al–Si alloys at various extrusion conditions, which helps to select the extrusion parameters. As long as the extrusion force does not exceed the capacity of the press, the extrusion temperature can be further lowered to improve the surface quality of the extrusion and avoid surface cracking, which is caused by die friction and low material strength at high temperature.

The extrusions of the spray-formed hypereutectic Al–Si alloys in the shape of wires are shown in Fig. 7. The surfaces of the extrusions of AlSi18 and AlSi25 are very smooth, while the surface in the front section of the AlSi35 extrusion shows fine repetitive transverse cracks. Figure 7c, d shows that the cracks initiate in the surface region and propagate inward along the silicon particles. These cracks may result from either the hot shortness (fracture of large silicon particles) or longitudinal tensile stress exceeding the ultimate hot tensile strength at the surface of the billet under starting conditions of the extrusion process (at high temperature and high strain rate) [15]. After running up the process, transverse cracks in AlSi35 extrusions disappear, and only longitudinal grooves remain at the surface.

Figure 8 shows the microstructures of the extrusions of the spray-formed hypereutectic Al–Si alloys (longitudinal sections). The appearance of the silicon phase is similar to that of the as-deposited phase, while the distribution of the Si precipitations looks more homogeneous. In order to compare the silicon particle size of the as-deposited alloys with that of the as-extruded alloys, quantitative measurements of the silicon particle size before and after extrusion were made by means of image analysis (details can be found in another study) [25]. For the AlSi18, AlSi25, and AlSi35 deposits, the median equivalent diameter of the primary silicon particles is about 1, 3 and 11 μm, respectively. After extrusion, this diameter is about 2, 3 and 7 μm, respectively. The primary silicon particles in the AlSi18 alloy grow to a small extent, while the particles in the AlSi35 alloy suffer fracture after extrusion. This indicates that dislocation cannot bypass the comparatively large particles (>10 μm), and high stress concentration (dislocation pile-up) was generated at the particles and cause the particles to fracture during the heavy extrusion. Dislocations may bypass the comparatively small particles, and, thus, less external force is required to deform the

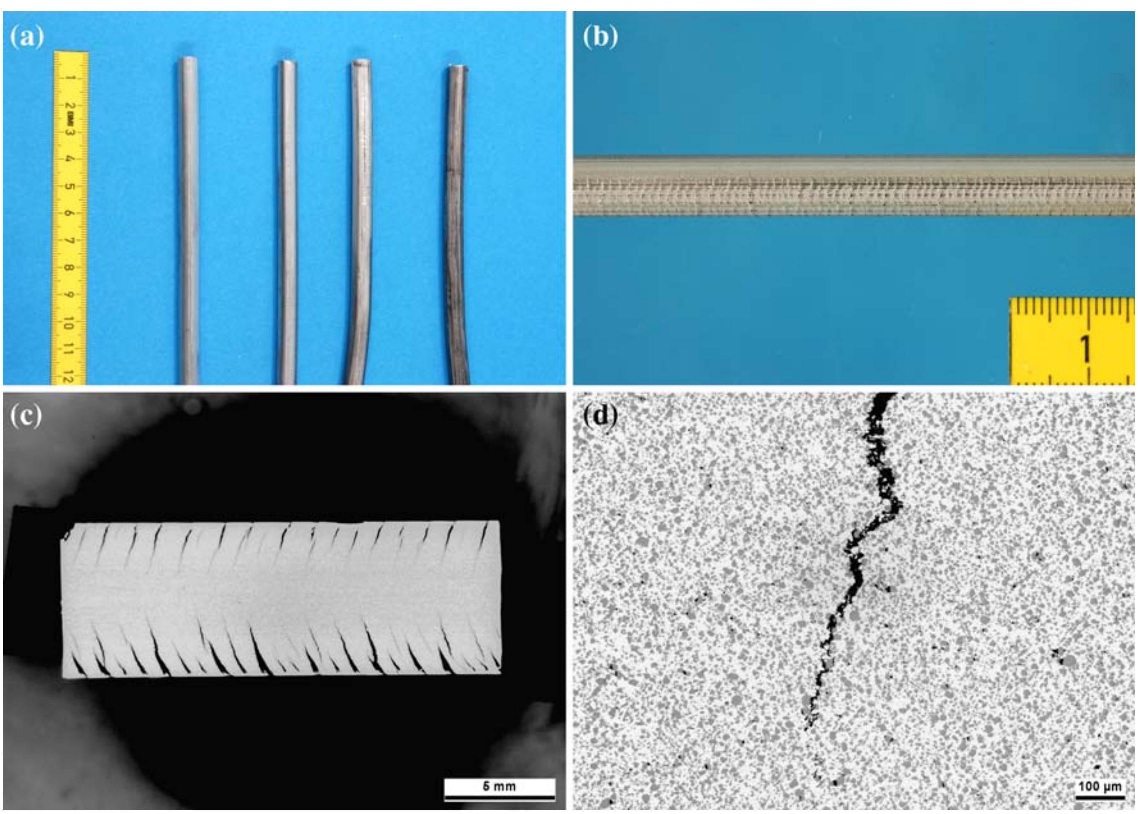

Fig. 7 Extruded wires from spray-formed hypereutectic Al–Si alloys: **a** from left to right: AlSi35 rear section, AlSi35 front section, AlSi25 and AlSi18; **b** repetitive transverse cracks in the front section of AlSi35; and **c**, **d** micrographs of the transverse cracks

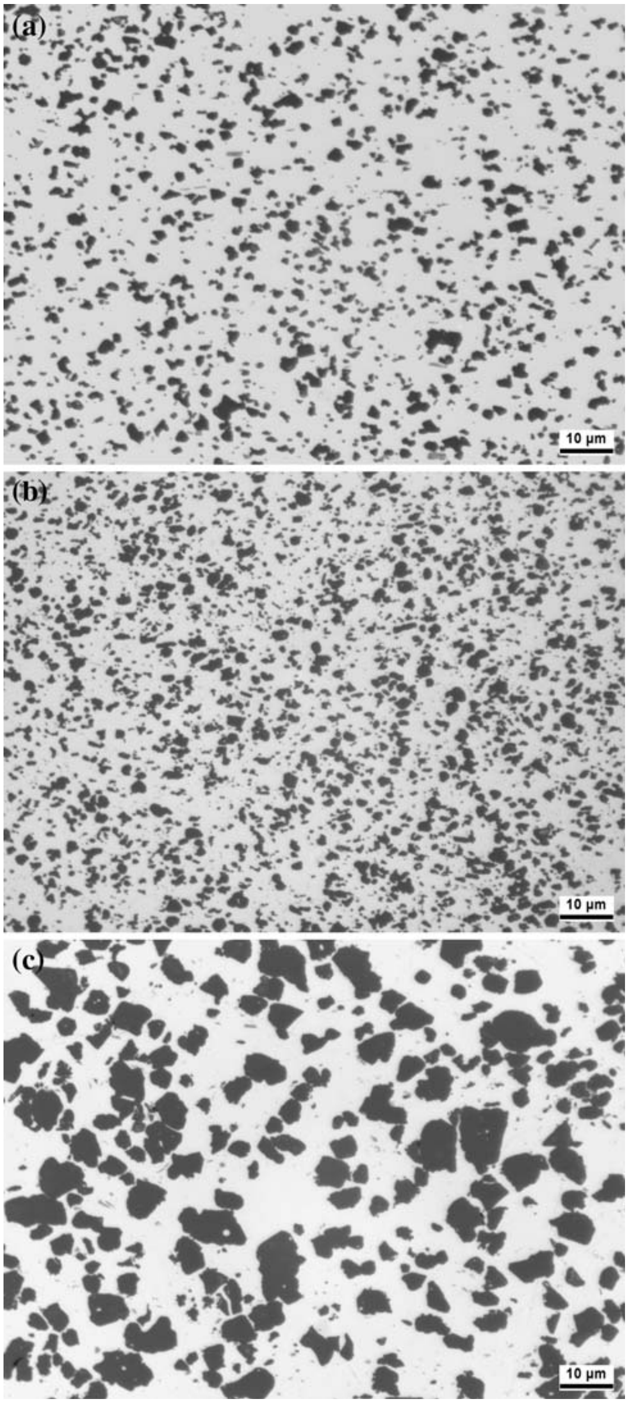

Fig. 8 Microstructures (longitudinal section) of extruded wires from spray-formed hypereutectic Al–Si alloys: **a** AlSi18; **b** AlSi25; and **c** AlSi35

materials. Porosity in the as-deposited materials (less than 1% in AlSi18 and AlSi25, around 3% in AlSi35) has been essentially reduced due to the heavy deformation. Only very few small pores have been found occasionally in the extrusions containing 35 wt% of silicon.

Summary and conclusions

(1) Compression tests have been conducted to obtain flow curves and to investigate the effects of strain rate, temperature, and material microstructure on the deformation behavior of the spray-formed Al–Si alloys. The flow stress of the spray-formed Al–Si alloys increases with decreasing compression temperature and increasing strain rate. Increasing silicon content in the alloys leads to higher flow stress in the deformation process. The strain rate sensitivity of the spray-formed Al–Si alloys increases from 0.06 to 0.18 as the compression temperature increases from 300 to 500 °C.

(2) The deformation of the spray-formed Al–Si alloys is controlled by two competing mechanisms: strain hardening and flow softening. In general, work hardening is the dominant mechanism in the beginning of the deformation and flow softening is more active in the later process. Only at high temperatures and low strain rates, work hardening is more pronounced than flow softening. High silicon alloys tend to show more significant flow softening. Particle damage during the deformation may have an influence on the flow curves of the alloys with large silicon particles.

(3) The spray-formed hypereutectic Al–Si alloy billets with a diameter of 107 mm after machining have been hot extruded into wires 8 mm in diameter. The area reduction ratio is about 189. Since primary silicon particles were greatly refined and uniformly distributed in the spray-formed materials, the heavy deformations of the spray-formed Al–Si alloys containing high amount of silicon were successfully performed.

Acknowledgements The authors gratefully acknowledge the financial support of the German Federal Ministry of Economics and Technology via the Federation of Industrial Research Associations (Arbeitsgemeinschaft industrieller Forschungsvereinigungen "Otto von Guericke" e.V.; AiF) within the program AiF-191ZN at the Foundation Institute for Materials Science (IWT) in Bremen. We also would like to thank our project partners for their beneficial contributions and valuable discussions on this study.

References

1. Hatch JE (1984) Aluminium, properties and physical metallurgy. American Society for Metals, Metals Park
2. Wu Y, Cassada WA, Lavernia EJ (1995) Metall Mater Trans 26A:1235
3. Yamauchi I, Ohnaka I, Kawamoto S, Fukusako T (1986) Trans Jpn Inst Met 27:195

4. Lavernia EJ, Wu Y (1996) Spray atomization and deposition. Wiley, New York
5. Grant PS (1995) Prog Mater Sci 39:497
6. Lawley A (2000) In: Bauckhage K, Uhlenwinkel V, Fritsching U (eds) Spray deposition and melt atomization SDMA 2000. University Bremen, Germany, p 3
7. Leatham AG (1999) Met Powder Rep 54:36
8. Grant PS (2007) Metall Mater Trans 38A:1520
9. Chiang CH, Tsao CYA (2006) Mater Sci Eng A 417:90
10. Chiang CH, Tsao CYA (2005) Mater Sci Eng A 396:263
11. Ha TK, Park WJ, Ahn S, Chang YW (2002) J Mater Process Technol 130–131:691
12. Hogg SC, Lambourne A, Ogilvy A, Grant PS (2006) Scr Mater 55:111
13. Johnston C, Crossley A (2004) MSTNEWS 4:14
14. Johnson W, Mellor PB (1973) Engineering plasticity. Van Nostrand Reinhold Company, London
15. Dieter GE (1988) Mechanical metallurgy. McGraw-Hill Book Company, New York
16. Davis JR (1993) ASM specialty handbook, aluminum and aluminum alloys. ASM International, Materials Park
17. McQueen HJ (1998) J Met 50(6):28
18. Prasad YVRK, Seshacharyulu T (1998) Int Mater Rev 43(6):243
19. Xia X, McQueen HJ (1997) Appl Compos Mater 4:333
20. Xiao BL, Fan JZ, Tian XF, Zhang WY, Shi LK (2005) J Mater Sci 40:5757. doi:10.1007/s10853-005-1292-5
21. Kouzeli M, Weber L, San Marchi C, Mortensen A (2001) Acta Mater 49:497
22. Kouzeli M, Weber L, San Marchi C, Mortensen A (2001) Acta Mater 49:3699
23. San Marchi C, Cao F, Kouzeli M, Mortensen A (2002) Mater Sci Eng A337:202
24. Tshätsch H (1987) Handbuch Umformtechnik: Arbeitsverfahren, Maschinen, Werkzeuge, Hoppenstedt-Technik-Tab.-Verl., Darmstadt
25. Cui C, Schulz A, Matthaei-Schulz E, Zoch HW (2009) J Mater Sci 44:4814. doi:10.1007/s10853-009-3734-y